Magnetic field effects on peristaltic flow of blood in a non-uniform channel

IOP Conf. Series: Materials Science and Engineering **263** (2017) 062019 doi:10.1088/1757-899X/263/6/062019

Magnetic field effects on peristaltic flow of blood in a non-uniform channel

R Latha and B Rushi Kumar
Department of Mathematics, School of Advanced Sciences, VIT University, Vellore-632014, India

E-mail: rushikumar@vit.ac.in

Abstract. The objective of this paper is to carry out the effect of the MHD on the peristaltic transport of blood in a non-uniform channel have been explored under long wavelength approximation with low (zero) Reynolds number. Blood is made of an incompressible, viscous and electrically conducting. Explicit expressions for the axial velocity, axial pressure gradient are derived using long wavelength assumptions with slip and regularity conditions. It is determined that the pressure gradient diminishes as the couple stress parameter increments and it decreases as the magnetic parameter increments. We additionally concentrate the embedded parameters through graphs.

1. Introduction

The transport of body fluids travelling through a flexible tube continuously by a progressive wave of relaxation and contraction due to a change of pressure along the walls like structure is called peristaltic pumping. Peristalsis is one of the important mechanisms for fluid in many biological situations. Peristalsis is a series of wave like contractions that moves food through the digestive tract. Peristalsis mixes and shifts the chime on the intestinal wall. In the digestive organ, water is assimilated into the circulatory system, at last, the staying waste items are discharged from the body through the rectum and anus. At the point when urine is expelled, the sphincter muscles get, the muscles of bladder relax and the urine is gathered again in the bladder. Eventually all the lymph vessels, including the lacteals coming from your small intestine, they all join up and they come up, your body and also the ones coming from the liver will merge and join and come up and travel up through the body. Spermatic flow in the ducts of the male reproductive tract, the movement of an ovum in Fallopian tube of the female reproductive system, the circulation of blood through small blood vessels and the locomotion of some warms. Some biomedical instruments like a roller, finger pumps, blood pump in the heart, lung machine are designed based on the peristaltic concept and also in moving of toxic and corrosive liquids to avoid pollution with the outside environment. Shapiro et al. [3] initiated the concept of long wave length and low Reynolds number approximation. Jaffrin et al. [1] and Manton [2] are analyzed the peristaltic transport with long wavelength at low Reynolds number. Colgan et al. [4] investigated with all Reynolds numbers on peristaltic transport of fluids. Barton et al. [5] discussed for long and short wave length peristaltic flow in tubes. T.W.Latham [6] only first investigated the peristaltic pumping in computational and experimental.

When we blend to added substances in the oil/fluid, the forces which are available in the fluid contradict the strengths of added substances, this resistance makes a couple forces and thus a couple stresses are prompted in the fluid. This type of fluid is known as couple stress fluid. Raghunath Rao et al. [7] concentrated the peristaltic movement of couple stress fluid saturated with suspended

particles. Brown et al. [8] examined the Reynolds number as finite and he only first attempted peristaltic transport of solid particle with fluid. Mekheimer et al. [10], Raghunatha Rao et al. [11], Chaturani [9], Sobh [12] have discussed couple stress fluid of peristaltic transport. Srivastava [13,14] has been researching the couple stress fluid as a genuine portrayal of the blood stream. These investigations are to examine the effect of MHD on peristaltic flow of a blood in a non-uniform channel. Stokes [15] only first developed the theory of couple stress fluid. El-Shehawy [16] concentrated that the fluids exhibit boundary slip have vital innovative applications, for example, in cleaning valves of the fake heart and inward cavities. Therefore a good understanding of the physical process of slip condition is necessary. Several researchers have been made on the subject of slip boundary conditions [17–29]. Slip effect exhibited two different types of fluids. The slip effect shows up in molten polymers, non-Newtonian fluids, and concentrated polymer solutions.

The inspiration of present work is slip effect on the peristaltic flow of blood under MHD in non-uniform channel have been extremely valuable in the part of peristaltic muscular contraction and transporting electrically conducting bio-fluid.

2. Formulation and solution of the problem

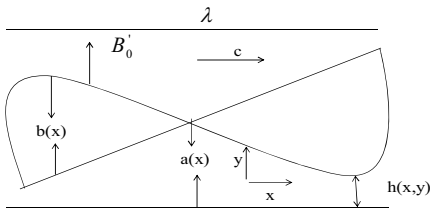

Figure 1 Geometry of the problem

Now we consider the peristaltic flow of electrically conducting couple stress fluid through a non-uniform channel with a sinusoidal wave going down its wall. Assumed to be the plates of the channel are electrically insulated and induced magnetic field is negligible. The shape of the flexible walls is represented by,

$$y = h(\mathrm{x},\mathrm{t}) = \mathrm{a}(\mathrm{x}) + \mathrm{b}\sin\frac{2\pi}{\lambda}(\mathrm{x}-\mathrm{ct}) \tag{1}$$

$$\text{With } a(\mathrm{x}) = \mathrm{a}_0 + kx \tag{2}$$

Here B_0' is acting along the y -axis, $a(x)$ is the mean half width of the channel, b is the peristaltic wave amplitude, c is the velocity of the peristaltic wave, a_0 is the half width at the inlet k is the constant whose magnitude depends on the length of the channel. λ is the wave length and t is the time.

The constitutive equations and equations of motion for a couple stress fluid are,

$$T_{ji,j} + \rho f_i = \rho\frac{\partial v_i}{\partial t}, \tag{3}$$

$$e_{ijk}\,T_{jk}^{A} + Ha_{ji,j} + \rho C_i = 0 \ , \tag{4}$$

$$\tau_{ij} = -p' + 2\mu d_{ij}\,, \tag{5}$$

$$\mu_{ij} = 4\eta\omega_{j,i} + 4\eta'\omega_{i,j}\,, \tag{6}$$

Associated with the couple stress η and η' are constant. p' is the pressure, f_i is the body for vector, C_i is the body moment. v_i is the velocity vector, w_i is the vorticity vector, μ_{ij} is the couple stress tensor, Ha_{ij} is the deviatoric part of Ha_{ij} , τ_{jk} is the symmetric part of stress tensor and T_{jk}^{A} is

the asymmetric parts of stress tensor T_{jk} respectively, d_{ij} is the symmetric part of the velocity gradient.

In the laboratory frame (X,Y) the governing equations of motion for MHD couple stress fluid are given by,

$$\frac{\partial u}{\partial x}+\frac{\partial v}{\partial y}=0 \tag{7}$$

$$\rho\left\{\frac{\partial u'}{\partial t'}+u'\frac{\partial u'}{\partial x'}+v'\frac{\partial u'}{\partial y'}\right\}=-\frac{\partial p'}{\partial x'}+\mu\nabla^2u'-\eta\nabla^4u'-\sigma'B_0^2u' \tag{8}$$

$$\rho\left\{\frac{\partial v'}{\partial t'}+u'\frac{\partial v'}{\partial x'}+v'\frac{\partial v'}{\partial y'}\right\}=-\frac{\partial p'}{\partial y'}+\mu\nabla^2v'-\eta\nabla^4v' \tag{9}$$

Where

$$\nabla^2=\frac{\partial^2}{\partial x'^2}+\frac{\partial^2}{\partial y'^2},\ \nabla^4=\nabla^2.\nabla^2$$

σ is electrical conductivity of the fluid where u' and v' are the velocity of the fluid particle B_0 is the applied magnetic field ρ is the density of the fluid.

The boundary conditions are

$$\frac{\partial u'}{\partial y'}=0,\ \frac{\partial^3u'}{\partial y'^3}=0 \text{ at } y'=0 \tag{10a}$$

$$u'=-\beta\frac{\partial u'}{\partial y'},v'=c\frac{\partial h'}{\partial x'}-\left(\frac{\partial^2v'}{\partial x'^2}-\frac{\partial^2u'}{\partial y'\partial x'}\right)\frac{\partial h'}{\partial x'}+\frac{\partial^2v'}{\partial y'\partial x'}-\frac{\partial^2u'}{\partial y'^2}=0\ \ at\ \ y'=h' \tag{10b}$$

$$x=\frac{x'}{\lambda},\ \ y=\frac{y'}{a_0},\ \ u=\frac{u'}{c},\ \ v=\frac{\lambda v'}{a_0c}$$

$$p=\frac{a_0^2}{\lambda\mu c}p'(\mathrm{x}'),\ \ t=\frac{ct'}{\lambda},\ \mathrm{Re}=\frac{\rho ca_0}{\mu},Ha=\sqrt{\frac{\sigma}{\mu}}B_0a_0,\ \ \ \delta=\frac{a_0}{\lambda},$$

$$h'=\frac{h'}{a_0}=1+\frac{\lambda kx}{a_0}+\phi\sin\{2\pi(\mathrm{x}-\mathrm{t})\} \tag{11}$$

Where $\phi=\frac{b}{a_0}<1$, β is slip parameter

The dimensionless form becomes

$$\frac{\partial u}{\partial x}+\frac{\partial v}{\partial y}=0 \tag{12}$$

$$\mathrm{Re}\ \delta\left\{\frac{\partial u}{\partial t}+u\frac{\partial u}{\partial x}+v\frac{\partial u}{\partial y}\right\}=-\frac{\partial p}{\partial x}+\nabla^2u-\frac{1}{S^2}\nabla^4u-Ha^2u \tag{13}$$

$$\mathrm{Re}\ \ \delta^3\left\{\frac{\partial v}{\partial t}+u\frac{\partial v}{\partial x}+v\frac{\partial v}{\partial y}\right\}=-\frac{\partial p}{\partial y}+\delta^2\nabla^2v-\frac{\delta^2}{S^2}\nabla^4v \tag{14}$$

$S=\sqrt{\frac{\eta}{\mu}}a_0$ is the couple stress fluid parameter, Ha is Hartmann number and δ is the wave number

The boundary conditions are

$$\frac{\partial u}{\partial y}=0,\quad \frac{\partial^3 u}{\partial y^3}=0 \text{ at } y=0 \tag{15a}$$

$$u=-\beta\frac{\partial u}{\partial y},\ v=\frac{\partial h}{\partial x}-\left(\delta^4\frac{\partial^2 v}{\partial x^2}-\delta^2\frac{\partial^2 u}{\partial y\partial x}\right)\frac{\partial h}{\partial x}+\frac{\partial^2 v}{\partial y\partial x}-\frac{\partial^2 u}{\partial y^2}=0 \text{ at } \quad y=h(\mathrm{x},\mathrm{t}) \tag{15b}$$

It follows the lubrication theory from Eq. (12) - (15) that the appropriate equations describing the flow

$$\frac{\partial p}{\partial x}=\frac{\partial^2 u}{\partial y^2}-\frac{1}{S^2}\frac{\partial^4 u}{\partial y^4}-Ha^2 u \tag{16}$$

$$\frac{\partial p}{\partial y}=0 \tag{17}$$

With dimensionless boundary conditions

$$\frac{\partial u}{\partial y}=0,\ \frac{\partial^3 u}{\partial y^3}=0 \text{ at } y=0$$

$$u=-\beta\frac{\partial u}{\partial y},\ \frac{\partial^2 u}{\partial y^2}=0 \text{ at } y=h(\mathrm{x},\mathrm{t})=1+\frac{\lambda k x}{a_0}+\phi\sin\{2\pi(\mathrm{x}-\mathrm{t})\} \tag{18}$$

$$u(\mathrm{x},\mathrm{y},\mathrm{t})=\frac{\partial p/\partial x}{Ha^2}\frac{(-n_2^2\cosh(n_2 h)\cosh(\mathrm{n}_1\mathrm{y})+\cosh(\mathrm{n}_2\mathrm{y})n_1^2\cosh(\mathrm{n}_1\mathrm{h}))}{(-n_2^2\cosh(\mathrm{n}_2\mathrm{h})[\cosh(\mathrm{n}_1\mathrm{h})+\beta\mathrm{n}_1\sinh(\mathrm{n}_1\mathrm{h})]+n_1^2\cosh(\mathrm{n}_1\mathrm{h})[\cosh(\mathrm{n}_2\mathrm{h})+\beta\mathrm{n}_2\sinh(\mathrm{n}_2\mathrm{h})])} \tag{19}$$

Where

$$n_1=\pm\frac{S}{\sqrt{2}}\sqrt{1+\left(1-\frac{4Ha^2}{S^2}\right)^{\frac{1}{2}}},\ n_2=\pm\frac{S}{\sqrt{2}}\sqrt{1-\left(1-\frac{4Ha^2}{S^2}\right)^{\frac{1}{2}}}$$

The volume flow rate $Q(x,t)$ is given by,

$$Q(\mathrm{x},\mathrm{t})=\int_0^h u(\mathrm{x},\mathrm{y},\mathrm{t})\ dy$$

$$Q(\mathrm{x},\mathrm{t})=\int_0^h[B(-N_1\cosh(\mathrm{n}_1\mathrm{y})+\mathrm{N}_2\cosh(\mathrm{n}_2\mathrm{y})-1)]\,\mathrm{dy}$$

Where $B=\frac{\partial p/\partial x}{Ha^2}$

$$\frac{dp}{dx}=\frac{QHa^2}{-\frac{N_1}{n_1}\sinh(\mathrm{n}_1\mathrm{h})+\frac{N_2}{n_2}\sinh(\mathrm{n}_2\mathrm{h})-\mathrm{h}} \tag{20}$$

3. Results and Discussions

3.1 Pressure gradient and volumetric flow rate:

To discuss the results of volume flow rate $Q(\mathrm{x},\mathrm{t})$, periodic in $(\mathrm{x}-\mathrm{t})$ $Q(x,t)=\bar{Q}+\phi\sin 2\pi(x-t)$

The constant value of $Q(x,t)$ gives the pressure gradient where $\bar{Q}$ is the time average of the flow over one period of the wave, ϕ is amplitude ratio, Ha is Hartmann number and the couple stress parameter is S. Where $a_0 = 0.01cm$, $L = \lambda = 10cm$, $k = 0.5a_0 / L = 0.0005$ dp/dx evaluated numerically.

3.2 The behaviour on different physical parameters on velocity:

Figure 2 and Figure 3 depicts that the velocity versus dimensionless time t and various values of couple stress parameter S and Hartmann number Ha for a non-uniform channel at fixed values $\beta = 0$, x =1, $y = 0$, dp/dx =0.5 and $\phi = 0.7$. As shown from Figure 2, a couple stress parameter increases as velocity decreases, moreover, the maximum values of the velocity are -3.2098, -4.8520, -6.0468 and -6.9560 for S =2, 3, 4 and 5 respectively at each of which occurs at *t*=0. It is observed that the velocity decreases by -53.86% when *S* increases from 2 to 5. From Figure 3 Hartmann number increases as the velocity increases, furthermore, the maximum values of the velocity are -6.9560, -6.4647, -6.0250, -5.6299 and -5.2733 for *Ha* = 0.20, 0.21, 0.22, 0.23 and 0.24 respectively at each of which occurs at t =0. It is observed that the velocity increases by 31.91% when Ha increases from 0.2 to 0.24. Figure 4shows that the velocity versus y for various values of S at fixed values $\beta = 0$, $x = t = \pi/4$, dp/dx =0.5 It is noticed that the velocity reduces as a couple stress parameter increases, moreover, the maximum values of the velocity are -2.7738, -4.3284, -5.4934, -6.3977 and -7.1233 for S =2, 3, 4, 5 and 6 respectively at each of which occurs at y =0. It is observed that the velocity decreases by -61.06% when *S* increases from 2 to 6.

3.3 The behaviour on different physical parameters on pressure gradient:

Figure 5 and Figure 7reveals that pressure gradient versus x the different physical parameters Hartmann number Ha, couple stress parameter S and slip parameter β at fixed values t=0, $\phi = 0.7$, $\bar{Q} = 1$,y=0, dp/dx=0.6 . As shown From Figure 5 Hartmann number increases as the pressure gradient dp/dx decreases, Furthermore the maximum values of the pressure gradient are 5.9756, 2.5210, -1.4015, -5.8059 and -10.7004 for Ha =3, 3.5, 4, 4.5 and 5 respectively at each of which occurs at *x*=0. It is observed that the pressure gradient reduces by -57.81% when *Ha* increases from 3 to 5. From Figure 6 couple stress parameter increases as the pressure gradient dp/dx decreases, Moreover, the maximum values of the pressure gradient are 5.9756, 0.7960, -2.0378, -3.7577 and -4.8805 for S =0.2, 0.25, 0.3, 0.35 and 0.4 respectively at each of which occurs at *x*=0. It is observed that the pressure gradient reduces by -86.68% when *S* increases from 0.2 to 0.4. From Figure 7 slip parameter increases as the pressure gradient dp/dx decreases, Furthermore, the maximum values of the pressure gradient are 5.9756, 1.9283, -0.3968, -1.9061 and -2.9649 for β = 5, 7, 9, 11 and 13respectively at each of which occurs at *x*=0. It is observed that the pressure gradient reduces by -67.73% when β increases from 5 to 13. Figure 8 and Figure 9depicts that pressure gradient versus dimensionless time t as Hartmann number Ha and couple stress parameter S at fixed values $\phi = 0.7$, $\bar{Q} = 1$, $y = 0$, dp/dx=0.6, $x = 1$, $\beta = 5$. As shown from Figure 8 Ha increases as the pressure gradient decreases, Moreover, the maximum values of the pressure gradient are -3.2026, -5.4495, -8.0300, -10.9470 and -14.2020 for Ha =3, 3.5, 4, 4.5 and 5 respectively at each of which occurs at t=0. It is observed that the pressure gradient reduces by -41.23% when Ha increases from 3 to 5. From Figure 9 couple stress parameter S increases as the pressure gradient decreases and the maximum values of the pressure gradient are -3.2026, -3.4565, -3.6770, -3.8695 and -4.0388 for S =0.2, 0.21, 0.22, 0.23 and 0.24 respectively at each of which occurs at t =0. It is observed that the pressure gradient reduces by -7.35% when *S* increases from 0.2 to 0.24.Figure 10 and Figure 11shows that pressure gradient versus time average of the flow $\bar{Q}$ as Hartmann number Ha and couple stress parameter S at fixed values $\phi = 0.7$, t =0, y =0, dp/dx =0.6, x=1, $\beta = 5$. As shown from Figure 10 Hartmann number Ha increases as the

pressure gradient decreases, Moreover, the maximum values of the pressure gradient are -4.4195, -5.0031, -5.6050, -6.2251 and -6.8635 for *Ha*=3, 3.1, 3.2, 3.3 and 3.4 respectively at each of which occurs at $\bar{Q}$ =1.4. It is observed that the pressure gradient decreases by -11.66% when *Ha* increases from 3 to 3.4. From Figure 11 couple stress parameter *S* increases as the pressure gradient decreases. The maximum values of the pressure gradient are -4.4195, -4.7700, -5.0742, -5.3400 and -5.5735 for S =0.2, 0.21, 0.22, 0.23 and 0.24 respectively at each of which occurs at $\bar{Q}$ =1.4. It is observed that the pressure gradient reduces by -7.35% when *S* increases from 0.2 to 0.24.Figure 12shows that pressure gradient versus Hartmann number as couple stress parameter S at fixed values $\phi = 0.7$, t=0, $y = 0$, dp/dx =0.6, $x = 1$, $\beta = 2$. It is noticed that with increasing values of S, the pressure gradient decreases. The maximum values of the pressure gradient are 0.0229, -0.5241, -0.9989, -1.4137 and -1.7782 for S =0.2, 0.21, 0.22, 0.23 and 0.24 respectively at each of which occurs at $Ha = 3.$ It is observed that the pressure gradient reduces by -47.53% when S increases from 0.2 to 0.24.Figure 13depicts that pressure gradient versus couple stress parameter as Hartmann number at fixed values $\phi = 0.7$, t=0, y =0, dp/dx =0.6, x =1, Ha =3, $\bar{Q}$ =1, $\beta = 2$ It is observed that increasing values of Ha, the pressure gradient decreases. The maximum values of the pressure gradient are -5.6523, -6.0923, -6.5459 and -7.0133 for Ha =3, 3.1, 3.2 and 3.3 respectively at each of which occurs at S =1. It is observed that thePressure gradient decreases by -7.22% when *Ha* increases from 3 to 3.3.

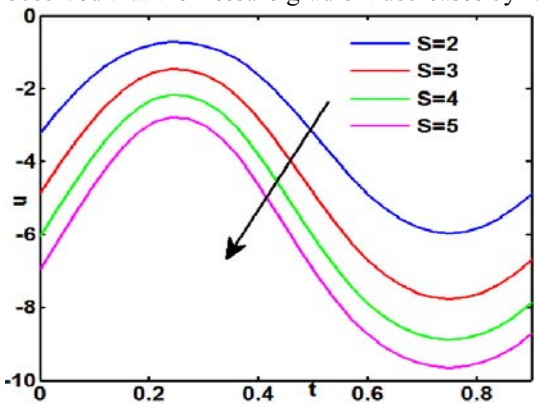

Figure 2.velocity distribution on different values of S at Ha =0.2.

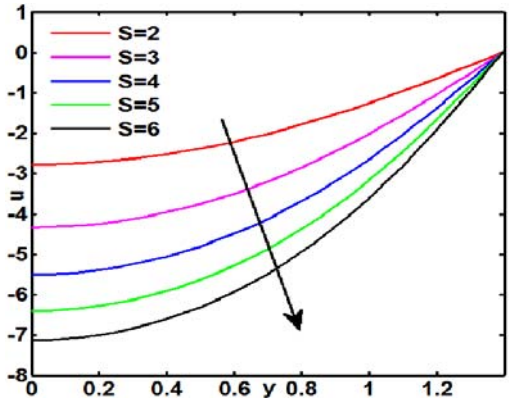

Figure 4. velocity distribution on different values of S at Ha =0.2.

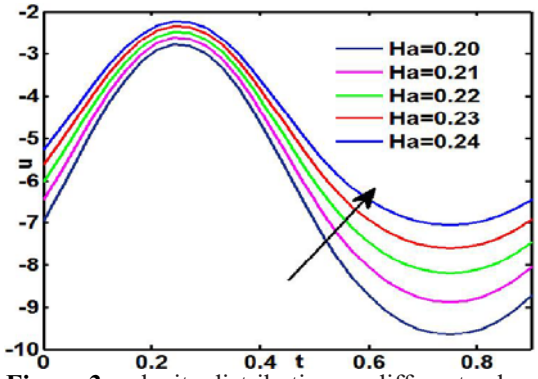

Figure 3. velocity distribution on different values of Ha at S =5.

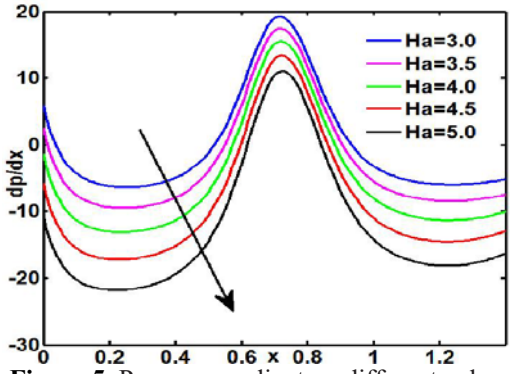

Figure 5. Pressure gradient on different values of Ha at S =0.2, $\beta = 5$

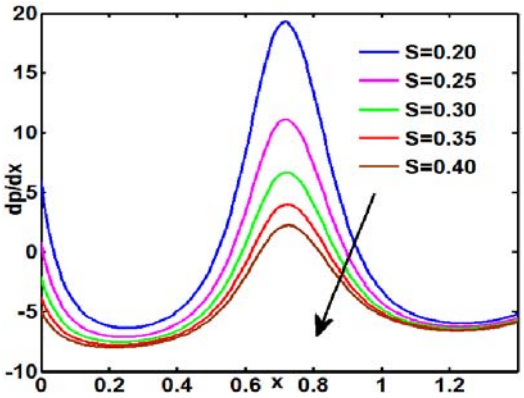

Figure 6. Pressure gradient on different values of S at Ha =3, β =5

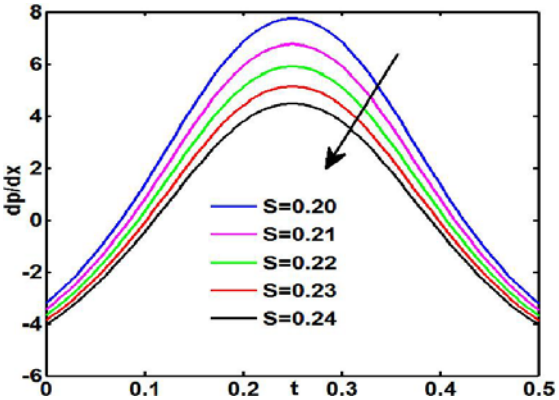

Figure 9. Pressure gradient on different values of S at Ha =3

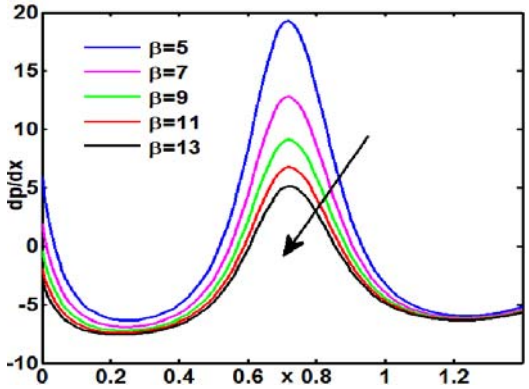

Figure 7. Pressure gradient on different values of β at Ha =3, S =0.2

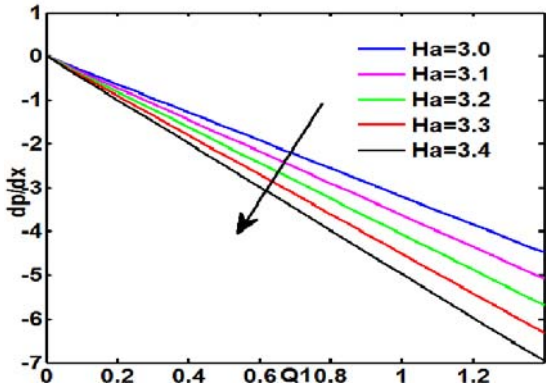

Figure 10. Pressure gradient on different values of Ha at S =0.2

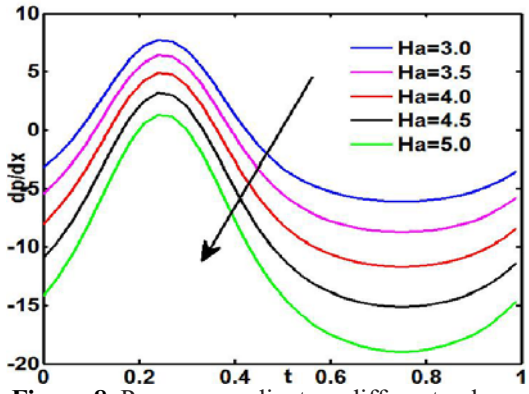

Figure 8. Pressure gradient on different values of Ha at S =0.2

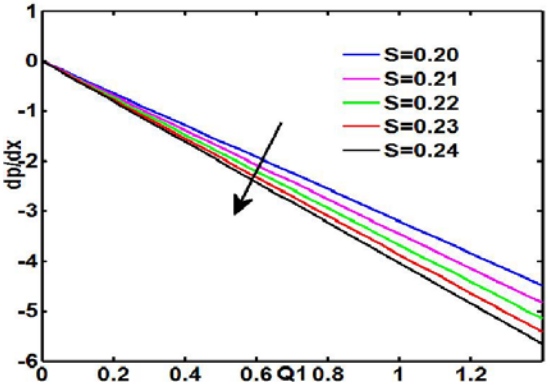

Figure 11. Pressure gradient on different values of S at Ha =3

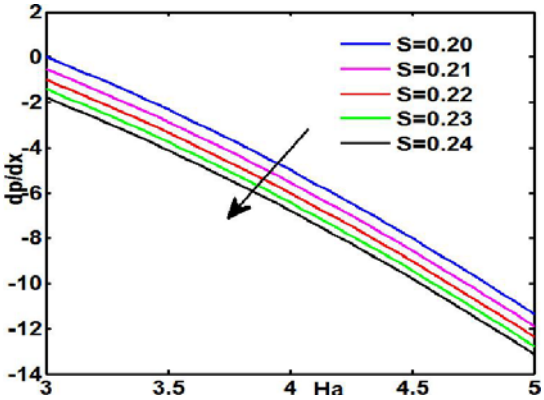

Figure 12. Pressure gradient on various values of S at $\overline{Q}$ =1

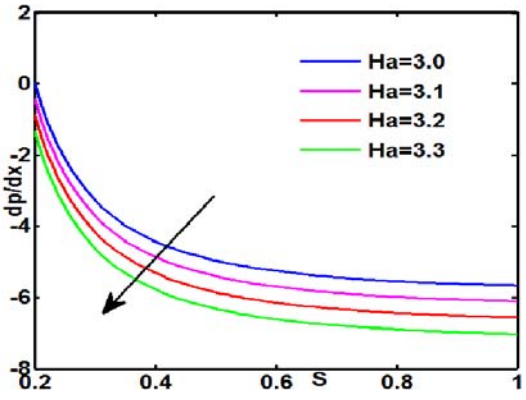

Figure 13. Pressure gradient on different values of Ha

4. Conclusions

The slip condition and the influence of magnetic field on the peristaltic flow of blood under lubrication approach have been discussed. Peristaltic flows with the interaction of various emerging parameters are studied with the help of illustrations. We conclude with some interesting notices have been revealed:

- The velocity versus t reveals that the couple stress parameter increases as the velocity decreases. The velocity versus y have the same behavior compared to the velocity versus t
- The pressure gradient versus t shows that the Hartmann number raises as the pressure gradient decreases. The velocity versus t has the same periodic wave trend, but it has opposite behavior compared to the pressure gradient versus t.
- The effect of pressure gradient with Hartmann number and the effect of pressure gradient with couple stress parameter have the same behavior.
- The pressure gradient versus x depicts that the pressure gradient reduces as increasing the slip parameter.
- The effect of S and Ha on the pressure gradient versus flow rate where the Hartmann number and the couple stress parameter increases as pressure gradient decreases.
- The pressure gradient versus Hartmann number depicts that couple stress parameter increases as the pressure gradient decreases. The pressure gradient versus heat source parameter shows that the Hartmann number increases as the pressure gradient reduces.

References

[1] Jaffrin M Y and Shapiro A H 1971*Ann. Rev. Fluid Dyns*.**3**13-37
[2] Manton M J 1975 *J. Fluid Mech* **68** 467 – 476
[3] Shapiro A H, Jaffrin M Y and Weinberg S L 1969 *J. fluid Mech*. **37** 799-825
[4] Colgan T and Terrill M R 1987*J. of Theoretical and Applied Mechanics* **6**3-22
[5] Barton C and Raynor S 1968*Biophys* **30** 663 – 680
[6] Latham T W 1966*MS Thesis*, *MIT Cambridge MA*.
[7] Raghunath Rao T and Prasada Rao D R V 2013*International Journal of Advances in Applied Mathematics and Mechanics* **1**8 6-102

[8] Brown T D and Hung T K 1977*Journal of Fluid Mechanics* **83** 249–272
[9] Chaturani P 1978 *Biorheology* **15** 119-128
[10] Mekheimer Kh S and Abd Elmaboud Y 2008*Physics Letters A* **372** 1657–1665
[11] Raghunatha Rao T and Prasada Rao D R V 2012 *Int. J. of Appl. Math and Mech.* **8** 97-116
[12] SobhA M 2008 Turkish *J. Eng. Sci* **32**117-123
[13] Srivastava L M 1985 *J. Biomech* **18** 479–485
[14] Srivastava L M 1986 *Rheol. Acta*. **25** 638–641
[15] Stokes V K 1966 *The Physics of Fluids.* **9**1709-1715.
[16] El-Shehawy E F, El-Dabe N T and El-Desoky I M 2006 *Journal of Acta Mechanica.* **186** 141–159
[17] Ali N, Hussain Q, Hayat T and AsgharS 2008*Physics Letters A* **372(9)** 1477-1489
[18] Hayat T, Qureshi M U and Ali N 2008*Physics Letters A*. **372(15)**2653–2664
[19] Sobh A M 2008*Turkish J. Eng. Envir. Sci* .**32** 117–123
[20] Sobh A M 2009*Canadian Journal of Physics* **87** 957–965
[21] Nadeem S and Akram S *2010 Int. J. Num. Meth. in Fluids* **63** 374–394
[22] El-Shahed M 2003 *App. Math. Comp.* **138** (2-3) 479–488
[23] Eldesoky I M 2012*Int. J. Math. Math. Sci.* **2012** 1**-**26
[24] Eldesoky I M, Kamel M H and Abumandour R M 2014*World J. Eng.and Tech.* **2**131–148
[25] Akram S 2014 *Computational Mathematics and Mathematical Physics*, **54** 1886–1902
[26] Safi A, Nadeem S and Hussin A 2014*Iranian Journalof Chemistry and Chemical Engineering* **33** 43–52
[27] Mekheimer Kh S 2004*Applied Mathematics and Computation* **153** 763–777
[28] Lakshminarayana P, Sreenath S, Sucharitha G 2015 *Procedia Engineering***127** 1087-1094
[29] Satyanarayana K V V, Sreenadh S, Sucharitha G and Lakshminaryana P 2016 *Indian J. Sci. and Tech.* **9** 1-9